Original Article
Environmental Health and Toxicology
Volume: 26, Article ID: e2011017: 7 pages
http://dx.doi.org/10.5620/eht.2011.26.e2011017 eISSN 2233-6567

EHT
Open Access

Apoptosis Induced by Manganese on Neuronal SK-N-MC Cell Line: Endoplasmic Reticulum (ER) Stress and Mitochondria Dysfunction

Hyonok Yoon[1,3], Do-Sung Kim[1], Geum-Hwa Lee[1], Kee- Won Kim[1], Hyung-Ryong Kim[2], Han-Jung Chae[1]

[1]Department of Pharmacology, School of Medicine, Chonbuk National University, Jeonju, Korea; [2]Dental School, Wonkwang University, Iksan, Korea; [3]School of Pharmacy, Howard University, Washington DC, USA.

Objectives: Manganese chloride ($MnCl_2$) is one of heavy metals for causing neurogenerative dysfunction like Manganism. The purpose of this study was to determine the acute toxicity of $MnCl_2$ using different times and various concentrations including whether manganese toxicity may involve in two intrinsic pathways, endoplasmic reticulum (ER) stress and mitochondria dysfunction and lead to neuronal apoptosis mediated by organelle disorders in neuroblastoma cell line SK-N-MC.
Methods: In the acute toxicity test, five concentrations (200, 400, 600, 800, 1,000 uM) of $MnCl_2$ with 3, 6, 12, 24, 48 hours exposure were selected to analyze cell viability. In addition, to better understand their toxicity, acute toxicity was examined with 1,000 uM $MnCl_2$ for 24 hours exposure via reactive oxygen species (ROS), mitochondria membrane potential, western blotting and mitochondrial complex activities.
Results: Our results showed that both increments of dose and time prompt the increments in the number of dead cells. Cells treated by 1,000 μM $MnCl_2$ activated 265% ($\pm$8.1) caspase-3 compared to control cell. $MnCl_2$ induced intracellular ROS produced 168% ($\pm$2.3%) compared to that of the control cells and $MnCl_2$ induced neurotoxicity significantly dissipated 48.9% of mitochondria membrane potential compared to the control cells.
Conclusions: This study indicated that $MnCl_2$ induced apoptosis via ER stress and mitochondria dysfunction. In addition, $MnCl_2$ affected only complex I except complex II, III or IV activities.

Key words: Apoptosis, Endoplasmic reticulum stress, Manganese chloride ($MnCl_2$), Mitochondria dysfunction

INTRODUCTION

Neurodegenerative diseases increasingly prevail in our communities recently due to several causes such as aging, heritage and heavy metals exposures. Manganese chloride ($MnCl_2$) is one of heavy metals for causing neurogenerative dysfunction which is similar to but somewhat different from idiopathic Parkinson's disease (PD) [1].

$MnCl_2$ is widespread in our everyday environment and plays pivotal roles in many functions. Required amount of $MnCl_2$ can be beneficial for living organisms through regulating enzymatic synthesis and promoting hematopoiesis [2,3]. It is also a fundamental ingredient for making fungicides, steel, and welding metals and many industry products [4]. However, overexposure to $MnCl_2$ may cause neural dysfunction in humans. The symptoms are bradykinesia, rigidity, tremor [5] which are the same sort of those in PD. The mechanism of cell death induced by $MnCl_2$ toxicity have not been understood clearly so far though several hypothesis of Endoplasmic Reticulum (ER) stress and mitochondria disorders have been reported.

The ER stress has been known to play a role in many neurodegenerative diseases as well as other diseases. It is caused from the accumulation of excessive unfold protein response (UPR) which leads to cell apoptosis [6]. Apoptosis due to ER stress has two main pathways, transcription pathway and a caspase dependent factor.

The malfunctioning of Mitochondria is associated with a number of neurodegenerative diseases as much as ER stress. Mitochondria are often called "cellular power plants" since it generates most of the cell supply of adenosine triphosphate

Correspondence: Han-Jung Chae, PhD
567 Baekje-daero, Deokjin-gu, Jeonju 561-756, Korea
Tel: +82-63-270-3092, Fax: +82-63-275-2855
E-mail: hjchae@chonbuk.ac.kr

Received: Aug 20, 2011, Accepted: Nov 11, 2011, Published Online: Dec 20, 2011
This article is available from: http://e-eht.org/

(ATP), an important energy source, which is involved in the control of cell cycle and cell growth [7] as well as cell signaling, cellular metabolism and cell death. Also, Mitochondria play a critical role in many metabolic systems such as regulation of membrane potential [8], apoptosis-programmed cell death [9,10]. It can transiently store calcium for the cell homeostasis which is primarily driven by mitochondrial membrane potential [11]. Mitochondria may leak some amount of high-energy electrons in the respiratory chain to form reactive oxygen species (ROS). This can lead to mutate mitochondrial DNA after resulting in significant oxidative stress in the mitochondria.

In this paper, we investigate whether ER stress and mitochondria malfunction would be related to $MnCl_2$ toxicity.

MATERIALS AND METHODS

I. Materials

Dulbecco's modified eagle medium (DMEM), fetal bovine serum (FBS), trypsin, and other tissue culture reagents were purchased from Life Technologies, Inc. (Gaithersburg, MD, USA) $MnCl_2$, sucrose, 4-(2-hydroxyethyl)-1-piperazineethanesulfonic acid (HEPES), ethylene diamine tetra acetic acid (EDTA) and other reagents were purchased from Sigma. 3, 3-dihexyloxacarbo-cyanine iodide ($DiOC_6$) and 2, 7-dichlorofluorescin diacetate (DCF-DA; Molecular Probes) were from molecular probes (Eugene, Oregon, USA). All of the other chemicals were purchased from either Sigma or Aldrich (St. Louis, MO, USA) and stored according to the manufacturer's instructions. All reagents were of analytical grade, and plastic wares were obtained from Falcon Inc. (Franklin, NJ, USA). GRP78, C/EBP homologous protein (CHOP), β-actin were purchased from Santa Cruz Biotechnology (Santa Cruz, CA, USA). Phosphorylated eukaryotic initiation factor 2α (p-eIF-2α) was provided by Cell Signaling Technology Inc. (Danvers, MA, USA)

II. Cell Culture and Viability

SK-N-MC human neuroblastoma cells were obtained from the American type culture collections (Manassas, VA, USA). The SK-N-MC neuroblastoma cell lines were maintained in DMEM containing 10% (v/v) heat-inactivated FBS, penicillin G (100 U/mL), streptomycin (100 mg/mL), and L-glutamine (2 mM). Cell viability was assessed with the trypan blue exclusion assay and calculated by dividing the non-stained (viable) cell count by the total cell count (3×10^6).

III. Fluorescent Staining of Nuclei

For apoptosis studies, the experiments were performed after treating SK-N-MC cells with $MnCl_2$. In the cells, nuclei were stained with chromatin dye (Hoechst 33258). Briefly, cells were fixed with 3.7% paraform aldehyde for 10 minutes at room temperature, rinsed twice 5 minutes with PBS, and incubated with 10 μM Hoechst 33258 in PBS at room temperature for 30 minutes. After three washes in PBS, the cells were observed under a fluorescence microscope (MPS 60, Leica). Morphological changes of nuclei were observed under a fluorescence microscope. To evaluate apoptotic cell death, Hoechst 33258 was used to visualize nuclear morphology and the number of cell death was counted.

IV. Determination of Caspase-3 Activity

The SK-N-MC cells (3×10^6) were washed with PBS and incubated for 30 minutes on ice with 100 mL of a lysis buffer (10 mM Tris-HCl, 10 mM NaH_2PO_4/$NaHPO_4$, pH 7.5, 130 mM NaCl, 1% triton1 X-100, and 10 mM sodium pyrophosphate). The cell lysates were spun, the supernatants were collected and the protein concentrations were determined using the BCA method. For each reaction, 30 μg of protein was added to 1 mL of a freshly prepared protease assay buffer (20 mM HEPES pH 7.5, 10% glycerol, 2 mM dithiotreitol) containing 20 mM of AC-DEVD-AMC (N-acetyl-Asp-Glu-Val-Asp-7-amino-4-methylcoumarin) (BD Biosciences Pharmingen).

The reaction mixtures in the absence of cellular extracts were used as the negative controls (fluorescence background). The reaction mixtures were incubated for 1 hour at 37˚C, and the level of aminomethyl-coumarin liberated from AC-DEVD-AMC was recorded using a spectrofluorometer (Hitachi F-2500) at an excitation wavelength of 380 nm and an emission wavelength range of 400-550 nm. The data were recorded as the integral of the relative fluorescence intensity minus the background fluorescence.

V. Cytofluorometric Assessment of Mitochondrial Membrane Potential

Mitochondrial membrane potential was measured as described in [12]. Briefly, a stock solution of $DiOC_6$ (4 mM/L) was prepared in ethanol and stored in small aliquot lots at -20˚C; working solution (dilution 1:2,000 for $DiOC_6$) was diluted in an experimental medium (DMEM) immediately before use. A total of 5×10^5 cells were incubated in DMEM that contained 100 nM $DiOC_6$ at 37˚C, and were analyzed using a PAS cytofluorometer (Partec, Münster, Germany) equipped with Partec software. Forward and side scatters were gated for the major population of normally sized cells and a minimum of 10,000 cells were analyzed. The fluorescent probe $DiOC_6$ was excited using a 488 nm argon laser, and emissions were collected through an FL1 detector fitted with a 525 ± 5 nm band pass filter.

VI. DCF-DA assay

For measuring ROS, DCF-DA assay was performed as described [12]. The cells were incubated with 1 mM $MnCl_2$ for 24 hours. After harvest, cells were treated with 100 μM DCF-DA at 37˚C for an additional 30 minutes. After chilling on ice, cells were washed with cold PBS, were removed by scraping, and then were resuspended at 1×10^6 cells/mL in PBS containing 10 mM EDTA. The fluorescence intensities of DCF-DA formed by the reaction between DCF-DA and the intracellular ROS of >10,000 viable cells in each sample were analyzed by PAS Vantage flow cytometry (Partec, Münster, Germany) with 488 nm excitation and 525 nm emission. Data were collected and analyzed using Becton Dickinson Partec software. The experiments were repeated at least three times, and three experiments were included in the histogram data.

VII. Western Blotting Analysis

Cell lysates (50 μg of protein) were added to an equal volume of 3× sample buffer, heated to 98˚C for 5 minutes, and then separated by 10% SDS-polyacrylamide gel electrophoresis (SDS-PAGE). After electrophoresis, the proteins were transferred onto a nitrocellulose membrane using a semi-dry electrophoretic transfer system (BIO-RAD). The membrane was incubated in 5% dry milk at room temperature for 1 hour. The membranes were then incubated with the primary antibodies at room temperature for 2 hours. The antibodies were recognized using anti-mouse or anti-rabbit IgG1 secondary antibodies linked to horseradish peroxidase at room temperature for 60 minutes. The immunoreactive bands were visualized using an enhanced chemiluminescence (ECL) kit (Amersham) and exposed to LAS 3,000 (Fujifilm, Japan).

VIII. Preparation of Homogenates

Cells were harvested with trypsin and centrifuged at 3,000 ×g for 5 minutes at 4˚C. The pellet was washed 2 times with PBS and gently homogenized in buffer A (250 mM sucrose, 10 mM HEPES, 1 mM EGTA, 1 mM DTT, 2 mM $MgCl_2$, pH 7.4) with 40 uL/mL protease inhibitor and 10 uL/mL phosphatase inhibitor using a loose-fitting dounce (Teflon-glass) homogenizer. The homogenates were rapidly placed in eppendorf tubes and then centrifuged at 1,000 × g for 10 minutes at 4˚C to remove nuclei, debris, and unbroken cells. The supernatant was centrifuged at 1,000 × g for 5 minutes at 4˚C, and then the supernatant was centrifuged at 13,000 × g for 20 minutes at 4˚C to precipitate mitochondria.

IX. Mitochondrial Complex I Assay

Mitochondrial complex I activity was measured as described in [13] using the rotenone-sensitive rate of NADH oxidation (at 340 nm and 30˚C) with modification by Ragan [14]. The reaction mixture contained: 25 mM potassium phosphate pH 7.2, 0.2 mM NADH, 10 mM $MgCl_2$, 1 mM KCN, 2.5 mg fat-free BSA, and approximately 50 μg of protein in a final volume of 1 mL. The reaction was initiated by addition of CoQ1 (50 μM final concentration) and read at 340 nm against a blank containing all the components except CoQ1. After 5 minutes, 10 μL of 0.5 mM rotenone was added to the cuvettes and the inhibition rate was measured for additional 5 minutes.

X. Mitochondrial Complex II-III Assay

Mitochondrial complex II-III activity was measured as described [13] as the antimycin-A-sensitive rate of cytochrome c reduction (at 550 nm and 30˚C) using succinate as the substrate. The reaction mixture contained: 100 mM potassium phosphate pH 7.4, 0.3 mM potassium EDTA, 1 mM KCN, 100 μM cytochrome c, and approximately 50 μg of protein in a final volume of 1 mL. The reaction was initiated by addition of 20 μL of 1.0 M succinate. After the assay had run for 5-7 minutes, 10μL of antimycin- A (2 mg/mL) was added to test cuvettes and inhibited rate was measured for a further 5 minutes.

XI. Mitochondrial Complex IV Assay

Mitochondrial complex IV (EC 1.9.3.1) activity was measured as described [13] by the rate of cytochrome c oxidation (at 550 nm and 30˚C) using the method of Wharton and Tzagoloff [15].

The reference cuvette contained: 10 mM potassium phosphate pH 7.0, 50 μM reduced cytochrome c, and 1 mM potassium ferricyanide in a final volume of 1 mL. The test cuvette contained: 10 mM potassium phosphate pH 7.0 and 50 uM reduced cytochrome c. The reaction was initiated by adding approximately 25 μg of protein to the test cuvette. The first-order rate constant (k) was calculated from the difference between the natural logarithms of the absorbance at t = 0 and at three time points, 1, 2, and 3 minutes after adding the protein sample. The mean of these calculated values was then taken to be k and the activity expressed in k min-1 mg protein-1.

XII. Protein Determination

Protein concentrations of the homogenates were determined using the method of Lowry [16] with bovine serum albumin (BSA) as a concentration standard.

XIII. Statistical Analysis

Statistical comparisons were determined by the student's t

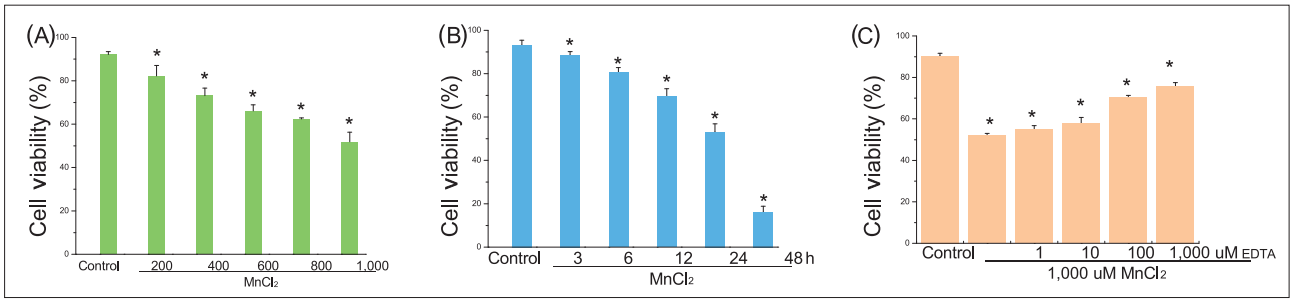

Figure 1. Cell death was assessed by Trypan Blue assay. (A) Cells were treated 200, 400, 600, 800, 1,000 μM $MnCl_2$ for 24 hours and the cell viability was assessed by trypan blue assay (control cells were treated without MnCl2). (B) Cells were treated with 1,000 μM $MnCl_2$ for 3, 6,12, 24, 48 hours and the cell viability was assessed by trypan blue assay. (control cells were treated without $MnCl_2$). (C) Cells were pretreated with 1,000 μM $MnCl_2$ 30minutes before followed by 1, 10, 100, 1,000 μM EDTA then incubated for 24 hours for cell viability.

Data represents mean ± standard error (n = 3).
*p < 0.05: significantly different from control cells.

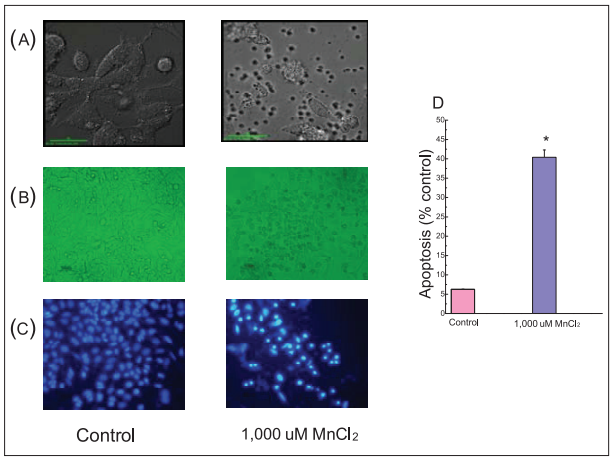

Figure 2. Cell morphology and apoptosis. (A) Cells were photographed with a confocal microscope. (B) Cells observed under a microscope after being treated with 1,000 μM $MnCl_2$ for 24 hours incubation. (C) The cells were stained with Hoechst 33258 and observed under a fluorescence microscope. (D) The shrinkage of nuclei and chromatin-condensed cells were quantified.

Data represents mean ± standard error (n = 3).
*p < 0.05: significantly different from control cells.

test for pair comparisons and by one-way ANOVA for multiple comparisons. Criterion for significance (p value) was set as mentioned in the figure legends.

RESULTS

1. $MnCl_2$-Induced Apoptosis Via ER Stress

To determine the relationship between ER stress and $MnCl_2$ toxicity, we examined cell viability including morphologic change via staining with Hoechst 33258 as wells as the expression of GRP78, CHOP, P-elf-2α. Figure1 A shows that that cell viability with 200 uM $MnCl_2$ is 82.26% (±4.86) but that with 1,000 uM $MnCl_2$ is 51.91% (±4.36). The results show that higher concentration of $MnCl_2$ decreases the cell viability. Figure 1B presents the relationship between cell viability and time, where three hours of exposure shows 88.57% (±1.60) of cell viability, however, they are 53.13% (±3.73) at 24 hours and 16.21% (±2.64) at 48 hours of $MnCl_2$ exposure, respectively. Exposure of 48 hours by $MnCl_2$ causes most of cells to be dead. Both increments of dose and time prompt the increments in the number of dead cells. These results lead to a conclusion that the cell death caused by $MnCl_2$ is dependent upon both dose and time. Figure 1C shows that cell viability with 24 hours $MnCl_2$ exposed is 51.98% (± 1.05) and that of pretreatment with EDTA shows 75.75% (±1.71); treatment with EDTA increases the cell viability about 147% compared to that of $MnCl_2$. This fact leads to a conclusion that EDTA is effective for the inhibition of the $MnCl_2$ -caused cell death.

We tested with 1,000 μM $MnCl_2$ for the next experiments to observe the apoptosis since necrosis takes place at higher concentrations of $MnCl_2$ [17]. The cells were incubated for 24 hours. It resulted in the death of almost all of cells (Figure 1B). Figure 2 presents nuclear shrinkage, an apoptotic parameter, which shows 40.4% (±1.9) of the apoptosis compared to control cells.

It was reported in the previous study [18] that ER stress induced by $MnCl_2$ occurred via the activation of multiple caspases. We performed experiments on the expression of an ER stress gene, GRP78 and p-elf-2α in SK-N-MC cells. The p-elf-2α is phosporylated pancreatic ER kinase RNA like ER kinase (PERK) which attenuates the initiation of translation in response to ER stress. Our experiment showed that 154% of GRP78, 420% of CHOP, 202% p-elf-2α expression were presented compared to each control (100%) (Figure 3).

One of proapoptic proteins, CHOP which facilitates the restoration of proper protein folding within the ER, initiates cell death through the activation of caspases. The report of

Morishima et al. [19] suggested that upon activation, caspase-12 translocates from the ER to the cytosol where it directly cleaves pro-caspase-9 which in turn activates the effecter caspase-3 [19]. In our experiment, caspase 3 activity protein is increased by 265±8.1% of the cell treated by 1,000 μM $MnCl_2$ compared to the control (Figure 4). Cells treated with 1,000 μM $MnCl_2$ clearly activated caspase-3 so that cell death was caused by apoptosis.

II. $MnCl_2$-Induced Apoptosis Via Mitochondria Dysfunction

We tested whether cell death induced by $MnCl_2$ was associated with mitochondria dysfunction through ROS generation, mitochondria membrane potential, mitochondria complex activities. Cells were treated with high dosage, 1,000 μM $MnCl_2$ and incubated for 24 hours to process the above experiments. Our study showed that $MnCl_2$ induced intracellular ROS produced 168% (±2.3%) compared to that of the control cells (100% on base line) (Figure 5) and $MnCl_2$ induced neurotoxicity significantly dissipated 48.9% of mitochondria membrane potential compared to the control cells (Figure 6).

Figure 7 presents that mitochondria complex I is decreased by 22.1±0.73% of the cells treated by $MnCl_2$. However, the cells treated by $MnCl_2$ do not affect complex II, III or IV activities. In intrinsic activation, cytochrome c from the mitochondria forms a complex with caspase-9, apoptosis-activating factor 1 (Apaf-1), and triggers caspase-9 activation. The activation of caspase-9 and ATP processes procaspase-3 [20-22]. Then, $MnCl_2$ toxicity causes also apoptosis induced mitochondria malfunction.

DISCUSSION

Our goal is to examine whether ER stress mediated processes may converge into intrinsic, mitochondrial pathway apoptosis in human blastoma SK-N-MC cells treated by $MnCl_2$.

It is known that cell death is normally caused by two mechanisms: necrosis and apoptosis. Necrosis is a mode of cell death that occurs under extremely physiological conditions to damage plasma membrane and makes plasma membrane to be evoked. Necrosis starts when cell homeostasis cannot be maintained and occurs with influx of water and extracellular constituents. It eventually leads to cell swelling and rupture in intracellular mitochondria.

However, apoptosis is a process for a cell to lead to its death from normal physiological conditions. It is related with two mechanisms such as ER stress and mitochondria dysfunction.

The ER stress due to the damage of Ca^{2+} homeostasis [23], inhibition of protein N-linked glycosylation, expression of mutant proteins cause the accumulation of misfolded

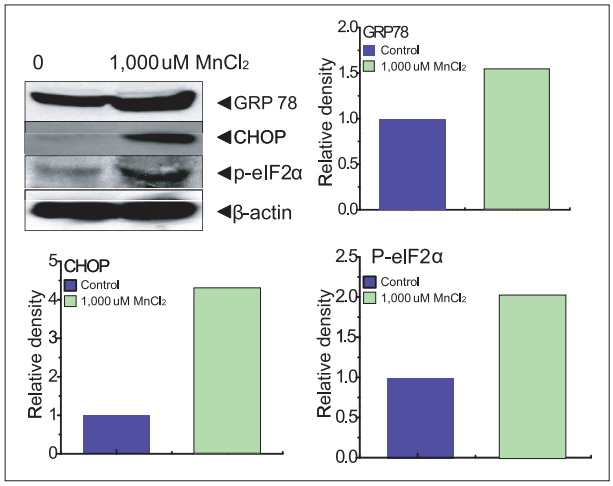

Figure 3. The cells treated with 1,000 μM $MnCl_2$ were lysed. SDS-PAGE and immunoblotting were performed with anti-GRP78, CHOP, p-eIF2, and β-actin.

Data represents mean±standard error (n=3).
SDS-PAGE: sodium dodecyl sulfate polyacrylamide gel electrophoresis, GRP78: glucose-regulated protein 78, CHOP: CCAAT/enhancer-binding protein (C/EBP) homology protein, p-eIF2: phosphorylated eukaryotic initiation factor.

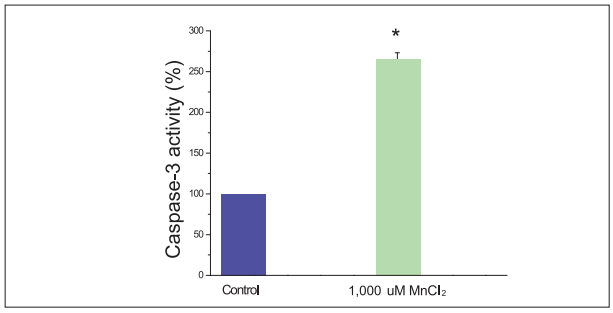

Figure 4. Cells were treated with 1,000 μM $MnCl_2$ for 24 hours and caspase-3 activity was measured.

Data represents mean±standard error (n=3).
*$p < 0.05$: significantly different from control cells.

proteins in the ER lumen [24]. The UPR alleviates ER stress with several factor such as induction of ER- chaperones, initiation of a degradation system and attenuation of protein synthesis [6]. One of ER-chaperones, GRP78 activates the cells treated by $MnCl_2$ (Figure 3). ER also is involved in stress-mediated apoptotic pathways, CHOP [25]. Figure 3 shows the expression of CHOP when the cell was treated with 1,000 μM $MnCl_2$ for 24 hours. The cells also activate p-eIF-2α which is one of proteins related with ER stress (Figure 3). The ER stress activates caspase-12, thereby triggering an ER-stress-specific cascade for implementation of apoptosis [26]. Also, when ER stress is prolonged, it may lead to the processing of the ER-resident protease procaspase-12 as well as the activation of calpain, caspase-3, caspase-6, and apoptosis in AD [26]. Administration of 1-Methyl-4-phenyl-1, 2, 3, 6-tetrahydropyridine (MPTP)

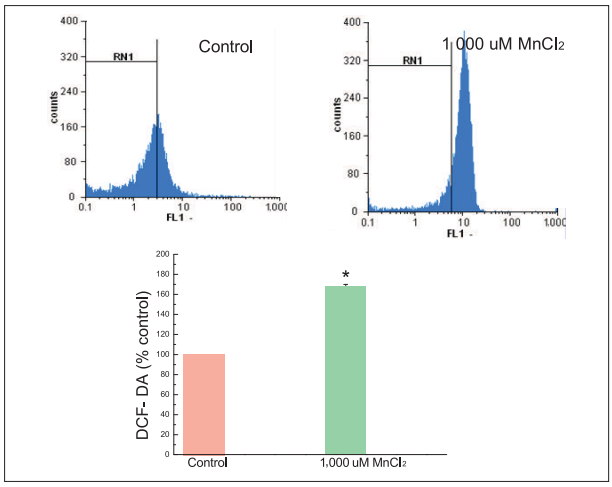

Figure 5. Intracellular ROS induced $MnCl_2$. Cells were treated with 1,000 μM $MnCl_2$ and were incubated with dichlorofluorescin diacetate (100 μ M), then the fluorescence intensities of 10,000 cells were analyzed by flow cytometry (Partec PAS). The DCFDA fluorescence was quantified.

ROS: reactive oxygen species, DCFDA: 2, 7-dichlorofluorescin diacetate.
*p < 0.05: significantly different from control cells.

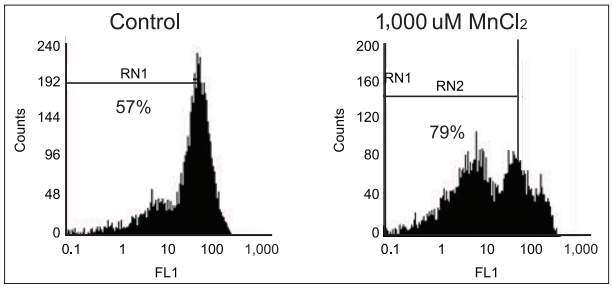

Figure 6. $MnCl_2$-induced mitochondrial membrane potential. Cells were treated with 1,000 μM $MnCl_2$ for 24 hours and then were incubated with $DiOC_6$ (100 nM). Fluorescence intensities of 10,000 cells were determines by flow cytometry (Partec PAS).

DiOC6: 3, 3 -dihexyloxacarbo-cyanine iodide.

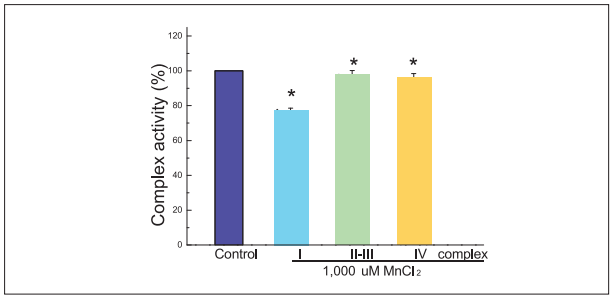

Figure 7. Complex I, II-III and IV activities expressed as a percentage of the control mitochondrial complex level in controls.

Data represents mean ± standard error (n = 3).
*p < 0.05: significantly different from control cells.

which causes a severe and irreversible Parkinsonian symptoms in humans induces activation of caspases, including caspase-3, 8, 9, and 11 [27-29]. Caspase-3 is activated in the apoptotic cell both by extrinsic death ligand and intrinsic mitochondrial pathways [30,31](Figure 4).

Mitochondria are the essential generators of intracellular ROS. Excessive production of ROS, formation of PTP, release of small proteins such as cytochrome c and apoptosis-inducing factor (AIF) cause mitochondria dysfunction, leading to trigger to initiate apoptosis. Released cytochrome c binds Apaf-1 and activates the caspase cascade, caspase-9 activation. Caspase-9 leads to stimulating activation of other caspases, such as caspase -3,-6,-7, which in turn head up a series of apoptotic events, finally leading to cell death [32-34].

In our experiment, Figure 5 shows the fact that $MnCl_2$ generates ROS spontaneously from mitochondria. $MnCl_2$ causes the dissipation of mitochondrial membrane potential (Figure 6) significantly by activating NADPH 314 K Oxidase. Also, $MnCl_2$ inhibits the activity of mitochondrial electron transport chain complex I (Figure 7) and decreases cellular ATP content.

Finally, $MnCl_2$ induces caspase-3 activity, a final executioner of apoptosis followed by cell death (Figure, 2B, 2C and 4).

Our finding about the different roles of $MnCl_2$-induced apoptosis may provide interesting insight into the mitochondrial and ER involvement in the process of different apoptotic programs. Caspase-3-dependent apoptosis of dopaminergic neurons might be also the essential catalyzing event that triggers subsequent progressive Manganism. Manganese toxicity can lead to neuronal apoptosis through the activation of intracellular apoptosis pathway. That means apoptosis might additionally contribute to the neural death in Manganism. But further studies might be necessary to uncover which other mechanisms are involved in the neural death in Manganism.

We hope this study would help further understanding of the cell death mechanisms in Manganism, particularly in regard to possible toxic effects impacted by occupational environment.

ACKNOWLEDGEMENTS

This work was supported by Korea Science and National Research Foundation (KRF-0029497) and the Korea Healthcare Technology R&D Project, the Ministry for Health, Welfare and Family Affairs (A 084144).

CONFLICT OF INTEREST

The authors have no conflict of interest to declare on this study.

REFERENCES

1. Aschner M, Guilarte TR, Schneider JS, Zheng W. Manganese: recent advances in understanding its transport and neurotoxicity. Toxicol Appl Pharmacol 2007; 221(2): 131-147.
2. Epperly MW, Sikora CA, DeFilippi SJ, Gretton JA, Zhan Q, Kufe DW, et al. Manganese superoxide dismutase (SOD2) inhibits radiation-induced apoptosis by stabilization of the mitochondrial membrane. Radiat Res 2002; 157(5): 568-577.
3. Sarikcioglu SB, Gumuslu S, Uysal N, Aksu TA. Plasma and erythrocyte magnesium, manganese, zinc, and plasma calcium levels in G-6-PD-deficient and normal male children. Biol Trace Elem Res 2004; 99(1-3): 41-47.
4. Olanow CW. Manganese-induced parkinsonism and Parkinson's disease. Ann N Y Acad Sci 2004; 1012: 209-223.
5. Barbeau A. Manganese and extrapyramidal disorders (a critical review and tribute to Dr. George C. Cotzias). Neurotoxicology 1984; 5(1): 13-35.
6. Xu C, Bailly-Maitre B, Reed JC. Endoplasmic reticulum stress: cell life and death decisions. J Clin Invest 2005; 115(10): 2656-2664.
7. McBride HM, Neuspiel M, Wasiak S. Mitochondria: more than just a powerhouse. Curr Biol 2006; 16(14): R551-R560.
8. Chaudry IH, Clemens MG, Baue AE. Alterations in cell function with ischemia and shock and their correction. Arch Surg 1981; 116(10): 1309-1317.
9. Green DR. Apoptotic pathways: the roads to ruin. Cell 1998; 94(6): 695-698.
10. Taylor SW, Fahy E, Zhang B, Glenn GM, Warnock DE, Wiley S, et al. Characterization of the human heart mitochondrial proteome. Nat Biotechnol 2003; 21(3): 281-286.
11. Siegel G, Walter A, Engel S, Walper A, Michel F. Pleiotropic effects of garlic. Wien Med Wochenschr 1999; 149(8-10): 217-224.
12. Kim DS, Kim HR, Woo ER, Hong ST, Chae HJ, Chae SW. Inhibitory effects of rosmarinic acid on adriamycin-induced apoptosis in H9c2 cardiac muscle cells by inhibiting reactive oxygen species and the activations of c-Jun N-terminal kinase and extracellular signal-regulated kinase. Biochem Pharmacol 2005; 70(7): 1066-1078.
13. Brooks KJ, Hargreaves IP, Bates TE. Nitric-oxide-induced inhibition of mitochondrial complexes following aglycaemic hypoxia in neonatal cortical rat brain slices. Dev Neurosci 2000; 22(5-6): 359-365.
14. Reed JS, Ragan CI. The effect of rate limitation by cytochrome c on the redox state of the ubiquinone pool in reconstituted NADH: cytochrome c reductase. Biochem J 1987; 247(3): 657-662.
15. Tzagoloff A, Wharton DC. Studies of the electron transport system. Lv. The influence of PH and of protein-depolymerizing reagents on the reaction of cytochrome a with borohydride. J Biol Chem 1964; 239: 582-585.
16. Lowry OH, Rosebrough NJ, Farr AL, Randall RJ. Protein measurement with the Folin phenol reagent. J Biol Chem 1951; 193(1): 265-275.
17. Liang Q, Zhou B. Copper and manganese induce yeast apoptosis via different pathways. Mol Biol Cell 2007; 18(12): 4741-4749.
18. Chun HS, Lee H, Son JH. Manganese induces endoplasmic reticulum (ER) stress and activates multiple caspases in nigral dopaminergic neuronal cells, SN4741. Neurosci Lett 2001; 316(1): 5-8.
19. Morishima N, Nakanishi K, Tsuchiya K, Shibata T, Seiwa E. Translocation of Bim to the endoplasmic reticulum (ER) mediates ER stress signaling for activation of caspase-12 during ER stress-induced apoptosis. J Biol Chem 2004; 279(48): 50375-50381.
20. Liu X, Kim CN, Yang J, Jemmerson R, Wang X. Induction of apoptotic program in cell-free extracts: requirement for dATP and cytochrome c. Cell 1996; 86(1): 147-157.
21. Porter AG, Janicke RU. Emerging roles of caspase-3 in apoptosis. Cell Death Differ 1999; 6(2): 99-104.
22. Katunuma N, Matsui A, Le QT, Utsumi K, Salvesen G, Ohashi A. Novel procaspase-3 activating cascade mediated by lysoapoptases and its biological significances in apoptosis. Adv Enzyme Regul 2001; 41: 237-250.
23. Boyce M, Yuan J. Cellular response to endoplasmic reticulum stress: a matter of life or death. Cell Death Differ 2006; 13(3): 363-373.
24. Kaufman RJ. Stress signaling from the lumen of the endoplasmic reticulum: coordination of gene transcriptional and translational controls. Genes Dev 1999; 13(10): 1211-1233.
25. Milhavet O, Martindale JL, Camandola S, Chan SL, Gary DS, Cheng A, et al. Involvement of Gadd153 in the pathogenic action of presenilin-1 mutations. J Neurochem 2002; 83(3): 673-681.
26. Takuma K, Yan SS, Stern DM, Yamada K. Mitochondrial dysfunction, endoplasmic reticulum stress, and apoptosis in Alzheimer's disease. J Pharmacol Sci 2005; 97(3): 312-316.
27. Hartmann A, Troadec JD, Hunot S, Kikly K, Faucheux BA, Mouatt-Prigent A, et al. Caspase-8 is an effector in apoptotic death of dopaminergic neurons in Parkinson's disease, but pathway inhibition results in neuronal necrosis. J Neurosci 2001; 21(7): 2247-2255.
28. Viswanath V, Wu Y, Boonplueang R, Chen S, Stevenson FF, Yantiri F, et al. Caspase-9 activation results in downstream caspase-8 activation and bid cleavage in 1-methyl-4-phenyl-1,2,3,6-tetrahydropyridine-induced Parkinson's disease. J Neurosci 2001; 21(24): 9519-9528.
29. Turmel H, Hartmann A, Parain K, Douhou A, Srinivasan A, Agid Y, et al. Caspase-3 activation in 1-methyl-4-phenyl-1,2,3,6-tetrahydropyridine (MPTP)-treated mice. Mov Disord 2001; 16(2): 185-189.
30. Salvesen GS. Caspases: opening the boxes and interpreting the arrows. Cell Death Differ 2002; 9(1): 3-5.
31. Ghavami S, Hashemi M, Ande SR, Yeganeh B, Xiao W, Eshraghi M, et al. Apoptosis and cancer: mutations within caspase genes. J Med Genet 2009; 46(8): 497-510.
32. Budihardjo I, Oliver H, Lutter M, Luo X, Wang X. Biochemical pathways of caspase activation during apoptosis. Annu Rev Cell Dev Biol 1999; 15: 269-290.
33. Dias N, Bailly C. Drugs targeting mitochondrial functions to control tumor cell growth. Biochem Pharmacol 2005; 70(1): 1-12.
34. Hengartner MO. The biochemistry of apoptosis. Nature 2000; 407(6805): 770-776.